# Chapter III: A Hybrid Micropattern Design for Supra-Oriented Cell Movement and Enhanced Multicellular Partitioning

## 1. Abstract

Geometrical constraints imposed by micropatterns affect cell motility. Micropatterned lines polarize cells and confine cell movement along a single axis.[1, 2] More recently, these line patterns have been shown to improve cell speed albeit the direction in which cells move along the line cannot be controlled.[3] Meanwhile, we and others have shown that teardrop-shaped micropatterns provide control over the direction of cell migration.[4, 5] As we begin to understand how specific micropatterned geometries affect cell motility, an emerging challenge is to mix and match pattern geometries to achieve multifaceted improvements in cell motility. Here, we show that the enhanced speed and persistence provided by line micropatterns and the directional control provided by the teardrop geometry may be combined in a new hybrid design to achieve rapid, directed cell movement. The hybrid micropattern increased the persistence and directional bias of cell movement compared to the standard teardrop geometry, revealing that combining geometric features can lead to unexpected synergistic improvements in cell motility. Using the hybrid micropattern as a polar bridge between two reservoirs, we show that cells may be selectively partitioned to one reservoir with approximately 85% enrichment within 36 hr.

## 2. Introduction

Physical cues from the surrounding environment can dictate cellular motility. For example, cancer cells can reorient surrounding ECM into parallel fibers that radiate outward from the tumor explants and can migrate along these fibers to facilitate metastasis.[6] Furthermore, there is emerging evidence that physically constrained environments, such as the blood and lymphatic vessels, promote cancer metastasis as well.[7] Researchers have tried to mimic such environments through micropatterning, and one such example is the line pattern.

Micropatterned lines have been used to guide axonal growth in neurons, aid blood vessel-like tissue formation, and study auto-reverse nuclear migration.[8-10] More recently, Yamada and colleagues found that cells on line patterns with sub-cellular widths can establish a uniaxial morphology with enhanced cell speed (unilamellar morphology).[3] However, if the lanes were too narrow, cell migration was hampered, and thus there was an optimum lane width for maximum cell speed.

Line patterns, however, do not permit control over the direction of cell movement. On the other hand, we and others have shown that teardrop-based micropatterns can be used to program the direction of cell movement.[4, 5] As we begin to understand better how micropattern features affect cell migration properties, it is intriguing to probe whether pattern features can be mixed and matched to achieve combinatorial enhancements in directed cell migration. Here, we sought to test whether a hybrid pattern that combines line and teardrop features might enable both rapid and directed movement.

## 3. Results

### *3.1. Line patterns markedly enhance persistence in addition to cell speed*

To begin to design our hybrid pattern, we first quantified cell movement of MCF-10A epithelial cells on micropatterned lines of different widths to determine the optimum line width for maximum cell speed. Consistent with previous studies,[3] we observed that the majority of MCF-10A cells established a migratory morphology with a single prominent lamella on one side of the cell when seeded on line patterns (unilamellar morphology; Chapter II Figure S2B). The cells moved ~40-50% faster on micropatterned lines than their counterparts on non-patterned surfaces that were prepared with identical chemistry (**Table 1**). The maximum cell speed was observed at an intermediate line width of 20 μm, above which the cells could no longer maintain the unilamellar morphology due to the lack of constraints at a single-cell width. The cells on thicker lines (30 μm and up) did not exhibit migration speed nor persistence length statistically different from that of non-patterned surface. Consistent with previous study with other cell lines,[3] there is an optimum width for maximum speed and it is 20 μm for MCF-10A cells.

Interestingly, we also observed significantly enhanced persistence upon confining MCF-10A cells to line patterns compared to cells on non-patterned surfaces. The cells with unilamellar morphology moved approximately 250-300 μm before flipping direction. In contrast, cells on a non-patterned surface moved only 50 μm on average before changing direction. As with cell speed, the optimum persistence length was observed on 20 μm-thick lines. Taken together, our observations show that both persistence and

migration speed enhancements correlate with the establishment of the unilamellar morphology.

| | Non-pattern | Line (5 μm) | Line (10 μm) | Line (20 μm) | Line (30 μm) |
|---|---|---|---|---|---|
| **Average persistence length (μm)** | 54 [12] | 253 [40] | 256 [57] | 310 [65] | 98 [41] |
| **Average migration speed (μm/hr)** | 55.5 [8.3] | 81.1 [12.0] | 87.4 [11.3] | 98.8 [14.7] | 60.9 [12.9] |
| **Fraction cells exhibiting unilamellar morphology** | 0% | 96% | 96% | 92% | 4% |

**Table 1.** Enhanced motility of MCF-10A epithelial cells on line patterns. Both the persistence length and cell migration speed are enhanced on line patterns, and are maximized on the thickest line. Unilamellar morphology was only observed on line patterns with widths below 20 μm. Persistence length is the distance cells travel before changing the direction 180° or breaking unilamellar morphology to spread. Migration speed includes the time they take to change directions. Values in the square brackets indicate standard error of the mean (n = 2-4).

*3.2. A hybrid micropattern design that combines line and teardrop features*

Although the 20μm line pattern provides significant enhancements to the speed and persistence of MCF-10A cell migration, this micropattern geometry provides no

control over the direction in which the cell travels. That is, the physical constraint imposed by the line geometry dramatically increases the tendency of cells to *maintain* a direction but does not bias cells to move preferentially up or down the line. In contrast, we and others have shown that teardrop-shaped micropatterns impart a directional bias to cell movement.[4, 5] MCF-10A cells preferentially hop from the tip end of a teardrop onto the blunt end of an adjacent island, leading cells to move in the counterclockwise direction (**Figure 1A**).

An intriguing hypothesis is that the effect of micropattern geometry on cell migration is modular. Such modularity would allow one to mix and match different micropattern shapes to achieve combinatorial enhancements in cell migration. To test this hypothesis, we designed a hybrid micropattern that blended the features of the line and teardrop geometries and quantitatively analyzed cell migration on this hybrid micropattern.

The hybrid design involved the insertion of a line segment of the optimum width (20 μm) between the blunt and tip ends of the standard teardrop pattern (**Figure 1B**). The hybrid design yields a spear-shaped pattern that maintains the blunt and tip ends, as these features were previously shown to play a key role in determining the directional bias with which cells hop from one micropatterned island to the next. Having hopped onto an island, cells would have to traverse the middle line segment to reach the other end. Since cells migrate with high persistence on line patterns, we reasoned that cells would successfully migrate across the line segment without turning back, provided that the length of the segment was significantly lower than the persistence length of cell

migration on line patterns (300 µm). Thus, the length of middle line segment was set at 100 µm.

To assess the effect of the hybrid micropattern on cell motility, we analyzed and compared the migration of MCF-10A cells on spear-shaped versus teardrop-shaped micropatterned islands. Both micropatterned islands were arranged to form a square-shaped "track" around which cells migrate. To ensure that any observed differences in migration could be attributed solely to the shape of the micropatterned island, the islands were arranged with precisely the same spacing and relative positioning. Time-lapse images were acquired of individual MCF-10A cells migrating on the square tracks, and the directional bias, persistence and speed of MCF-10A cell movement were quantified.

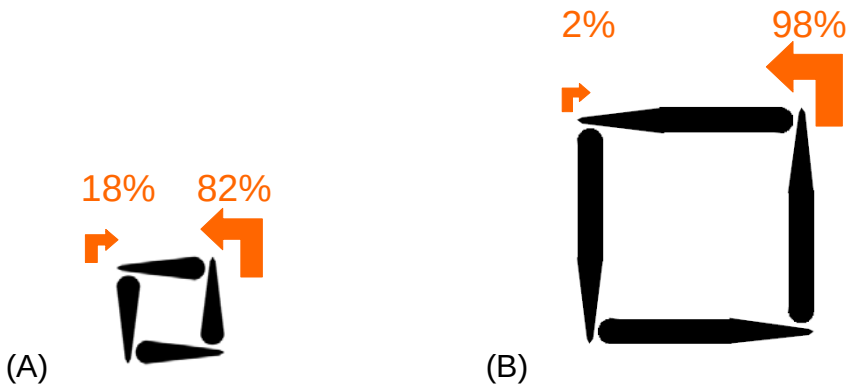


**Figure 1.** Schematic and directional bias of (A) teardrop and (B) spear-shaped patterns. Directional bias of spear-shaped patterns is greatly enhanced compared to the original teardrop patterns. Spear-shaped pattern has an extra 100 µm long, 20 µm wide line segment insertion in each of the teardrop islands (originally 80 µm long and 20 µm wide at blunt end).

*3.3. The hybrid spear-shaped micropattern markedly improves the directional bias of cell movement*

We first confirmed that the directional bias of cell migration exhibited on the original teardrop micropattern was not compromised by the addition of the middle line segment. Unexpectedly, cell migration on the hybrid spear-shaped micropattern exhibited even greater directional bias than on the original teardrop design. On the spear micropattern, cells moved from island to island with 98% of the hops favoring the blunt-to-tip direction, while only 2% of the successful hops occurred in the tip-to-blunt direction (**Figure 1B**). Meanwhile, on the standard teardrop-shaped micropattern, the bias for the blunt-to-tip hops was only 82% (**Figure 1A**).

To better understand this unexpected improvement in directional bias, we quantified the "decision" that cells make at each end of the spear- and teardrop-shaped micropatterns. On each end (tip or blunt), we quantified the likelihood that a cell hops to the adjacent island (successful hop) as opposed to "bouncing" by turning back to migrate down the island (**Table 2**). On the tip end of teardrop micropatterns, the hop probability was 73%. In contrast, the hop probability improved to 97% on the tip end of spear-shaped micropatterns. Furthermore, the likelihood that a cell hopped on the blunt end decreased from 38% on teardrop patterns to 15% on the hybrid spear patterns. Thus, the inclusion of a middle line segment in the teardrop pattern not only improved the likelihood of a hop at the tip end, but also reduced the probability that a cell would hop at

the blunt end. Thus, improvements in cell fate choices at both ends of the spear pattern together yield a marked enhancement in the directional bias of cell movement.

| Events at Corners | Occurrences for Teardrop | Occurrences for Spear | Average Residence Time for Teardrop (min) | Average Residence Time for Spear (min) |
|---|---|---|---|---|
| **Successful hop at tip end** | 208 (51.5%) | 166 (83.4%) | 30.7 | 28.5 |
| **Successful hop at blunt end** | 45 (11.1%) | 4 (2.0%) | 39.9 | 26.7 |
| **Bounce at tip end** | 78 (19.3%) | 6 (3.0%) | 48.9 | 28.5 |
| **Bounce at blunt end** | 73 (18.1%) | 23 (11.6%) | 50.6 | 41.4 |

**Table 2.** Detailed analysis of hop decisions at corners and residence times associated with the events. Events at each corner of the islands reveal the enhanced directional bias on the spear-shaped patterns. Residence times between the two patterns were statistically not different (except for residence time for bounce at tip end).

*3.4. Hybridizing line and teardrop micropatterns yields an additive improvement in the persistence of cell migration*

In addition to directional bias, our quantitative analysis showed that the tendency of cells to maintain the direction of movement increased on the hybrid spear micropattern compared to the original teardrop pattern. The average distance cells moved before

changing direction on the teardrop patterns was 383 μm. On the spear-shaped micropattern, the persistence length increased by 141% to 925 μm (**Table 3**). The observed increase in persistence was approximately equal to that expected by hybridizing a line segment and a teardrop pattern. Inserting a 100 μm line segment in an 80 μm teardrop would be expected to increase, the persistence by 125% to 862 μm, a value that differs only by 7% from the measured persistence of 925 μm. These results reveal that the line and teardrop shapes provide modular benefits to the persistence of cell migration, such that a hybrid pattern yields an approximately additive and predictable improvement in this aspect of cell migration.

| **Speed and Persistence** | **Teardrop** | **Spear** |
|---|---|---|
| **Average persistence length (μm) [a]** | 383 [230] | 925 [295] |
| **Average speed (μm/hr) [b]** | 91.0 [14.4] | 121.3 [14.2] |
| **Average net speed in the preferred direction (μm/hr) [c]** | 39.3 [31.6] | 92.9 [41.4] |

[a] Average persistence length corresponds to the average of distances cells traveled in the preferred direction without changing direction. [b] Speed corresponds to the total distance traveled divided by the total time. [c] Net speed corresponds to the net distance in preferred direction (distance in preferred direction – distance in opposite direction) divided by the total time.

**Table 3.** Cell motility on teardrop patterns and spear-shaped patterns. Speed and persistence are significantly enhanced on the spear-shaped patterns when compared to teardrop patterns. The differences between spear-shaped patterns and teardrop patterns

were statistically significant for all three parameters ($p < 0.01$; $n = 3$, more than 40 cells analyzed for each pattern). Values in the square brackets indicate standard error of the mean ($n = 2$-4).

*3.5. Reduced frequency of hops lead to improvements in migration speed on spear-shaped micropatterns*

Finally, we assessed the effect of inserting a line segment into the teardrop micropattern on cell migration speed. Since cell speed on line patterns is similar to that on teardrop patterns (98.8 on line and 91.0 μm/hr on teardrop), inserting a line segment into the teardrop pattern was not expected to affect cell migration speed. Quantitative analysis of time-lapse videos, however, revealed that the average cell speed on spear-shaped micropatterns was 121 μm/hr, a 33% improvement compared to teardrop micropatterns (**Table 3**).

To better understand this unexpected improvement in cell speed, we examined more closely the events at the corners of the square track where cells hop from one island to the next. We reasoned that the spear-shaped pattern may improve the average migration speed by reducing the amount of time for cells to hop at each corner. To test this possibility, we quantified the residence time of cells at the corners of the square track during tip-to-blunt and blunt-to-tip hops (**Table 2**). Residence times on spear-shaped patterns were on average shorter than those on teardrop patterns. The average residence times spent at the tip end were 29 min and 40 min on spear and teardrop patterns, respectively, while the times spent at the blunt end were 34 min and 46 min on spear and

teardrop patterns, respectively. Further analyses, however, showed these differences in hop duration were not statistically significant. Also, the residence times for U-turns were on average greater than residence times for successful hops at both ends of the island, but were mostly statistically not significant. These results revealed that the residence times at the corners of the square track were not statistically different between spear and teardrop patterns.

While differences in residence times do not contribute to the improvement in cell speed on spear patterns, this analysis raised an alternate hypothesis. With hops taking on average 37 min on spear and teardrop patterns, it consumes a significant fraction of the time a cell spends in traversing around the square track. For example, on a teardrop pattern, the cell takes 3.5 hr to traverse the track (320 μm ÷ 91 μm/hr) of which 2.8 hr is spent hopping at the corners. This observation taken together with the fact that hops occur more frequently on teardrop patterns (owing to their shorter length) may explain the improvement in average migration speed on spear shaped patterns.

To analyze this idea more quantitatively, we note that on the teardrop pattern, a hop decision must be made every 80 μm; in contrast, on the spear-shaped pattern, these decisions are spaced further apart (180 μm). Thus, the frequency of hops is approximately two fold greater on teardrop patterns. If we hypothetically insert an extra hop along a spear-shaped pattern, then the transit time along the spear would increase by 37 min or 0.6 hr from 180 μm ÷ 121 μm/hr = 1.5 hr to 2.1 hr. With this correction for hop frequency, the adjusted speed on spear-shaped patterns becomes 180 μm ÷ 2.1 hr =

86 μm/hr, a value that nearly matches the speed observed on teardrop-shaped pattern (91 μm/hr).

Therefore, we conclude that the hybrid spear-shaped micropattern improves cell migration speed not by enhancing cell migration or reducing the time it takes for cells to hop, but rather by requiring fewer hops per unit length owing to the insertion of a line segment in the base teardrop pattern. By inserting a line segment into the classical teardrop pattern, we exploit the remarkably high persistence of cell migration on line patterns. Thus, the directional bias conferred by each hop is capitalized over longer linear runs before the next junction is required to re-establish and maintain the bias in movement.

*3.6. Micropatterned bridges with hybrid patterns result in a rapid and effective partitioning across long distances*

As a step towards an application-oriented, high-order pattern to control cell population, we converted the highly biased spear-shaped patterns into a partition design. The spear-shaped patterns were extended in a zigzag fashion to bridge the two chambers separated by a 1000 μm distance (**Figure 3A**; note that the actual total distance of the spear-shaped bridge is 1500 μm long) and teardrop patterns were similarly converted into a bridge for comparison (**Figure 3B**; total distance of the teardrop bridge is 2268 μm long), while a simple straight line was used to connect the chambers for the control pattern (**Figure 3C**). We investigated the effectiveness of such micropatterned bridges in their ability to partition cell population between reservoirs.

Cells were uniformly seeded on the micropatterns and allowed to partition over a 36 hr period (**Figure 3D;** Supplementary Data **Movie 2**). Partition patterns incorporating the spear-shaped patterns effectively guided on average 85% of the cells towards the top half of the partition pattern and on average 60% of the cells into the top (preferred) chamber. Similarly, partition patterns with teardrop patterns effectively guided on average 79% of the cells towards the top half of the pattern and on average 51% of the cells into the top chamber. On the other hand, control patterns partitioned equally on both sides with 51% of the cells towards the top half and only 27% of the cells into the top chamber. Fractions were employed to account for the proliferation of cells.

We can also gain some insight into the partition dynamics as we follow the time course of observed partitioning every 3 hours. During the initial 0-6 hr period, the cells must become mobile and become unilamellar and thus the fraction of cells remains unchanged. During the next 9-24 hr period, there is a rapid flux of cells through the micropatterned bridges towards the upper chamber. However, as the top chamber is clogged with cells, it becomes increasingly difficult to move upwards. Likewise, as the bottom chamber is emptied, the rate of entrance into the bridge section becomes the rate-limiting step. As a result, the partition fraction reaches a plateau, which is less than the bias dictated by the previous spear-shaped pattern analysis.

t = 0 hr t = 36 hr

(A) Spear-Shaped Partition Pattern

Total distance per bridge = 1502 µm

Average partition at 36 hr = 84.7%

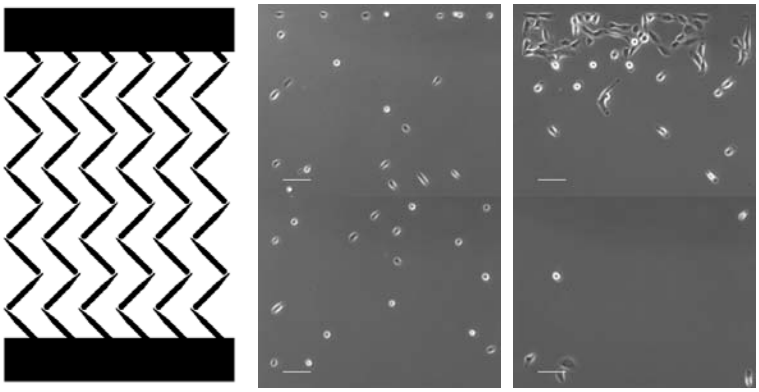

t = 0 hr t = 36 hr

(B) Teardrop Partition Pattern

Total distance per bridge = 2268 µm

Average partition at 36 hr = 79.4%

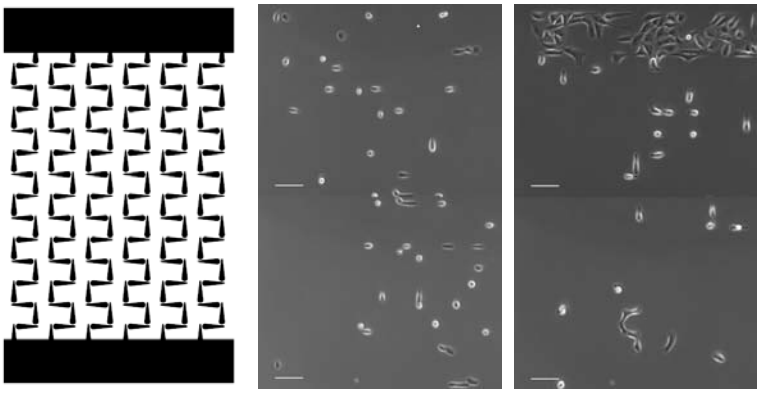

t = 0 hr t = 36 hr

(C) Control Pattern

Total distance per bridge = 1000 µm

Average partition at 36 hr = 51.1%

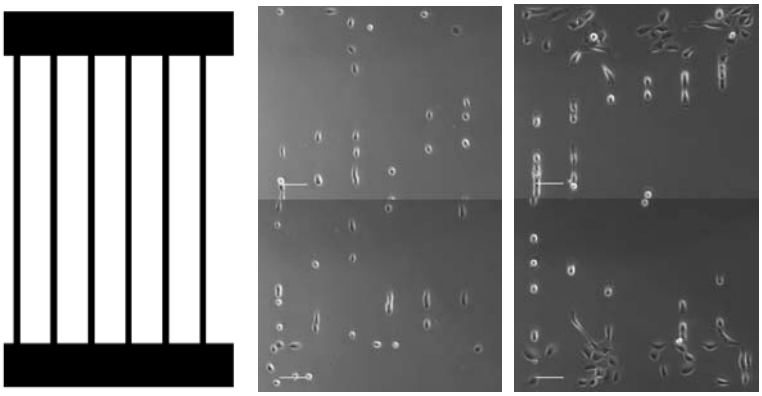

(D)

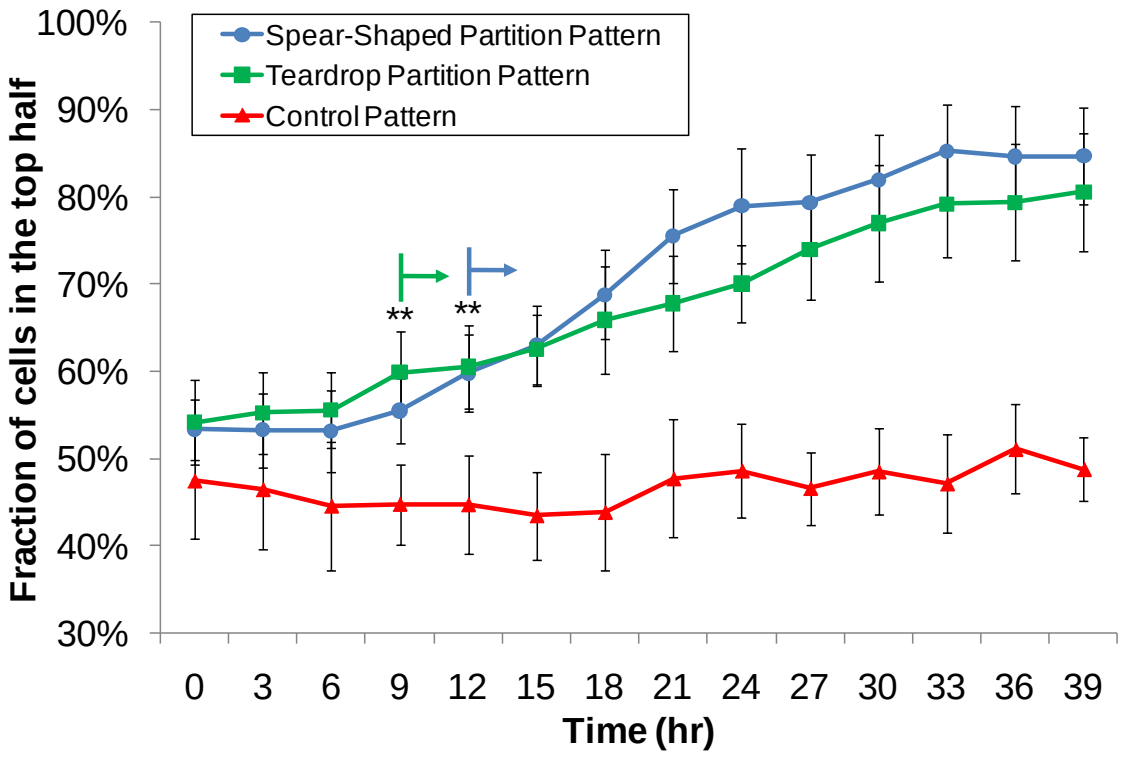


**Figure 3.** Schematic and effectiveness of partition patterns with spear-shaped and teardrop bridges. (A) The spear-shaped partition pattern and (B) the teardrop partition pattern guides the cells upwards, while (C) the control pattern does not [Scale bar = 100 μm]. (D) The fraction of cells in the top half of the pattern is plotted against time [**; $p<0.01$ (n=3, 8 patterns tested for each type)].

It is interesting to analyze the kinetics of partitioning in the multicellular context relative to the single-cell speeds measured in isolated spear-shaped patterns. The distance cells would have to travel through the bridge in the partitioning device is at most 1500 μm. Based on the observed single-cell net speed on spear-shaped patterns of 93

μm/hr, we can estimate that partitioning would occur in approximately 16 hr. However, it takes approximately 33 hr for partitioning to reach steady state after the initial 6 hr lag phase. This suggests that the rate of partitioning is retarded by phenomena not captured in the single-cell analysis. Such phenomena include cell-cell collisions, proliferation (as a side note, when a cell divides on a spear-shaped island, the two daughter cells initially migrate in opposite directions), island occupancy, etc. Consistent with the importance of multicellular phenomena in determining partitioning kinetics, we found that devices based on a teardrop bridge achieved the same extent of partitioning in a similar amount of time as a device based on spear patterns (**Figure 3D**). While the dynamics of multicellular behaviors are difficult to extrapolate solely from single cell migratory behavior, the effectiveness of the spear- and teardrop-based partitioning devices significantly surpass any previously reported micropattern-based partitioning.[11]

## 4. Conclusion

Geometrical constraints of micropatterns can govern cell motility. Some researchers have observed increased migration speed and persistence when cells are under width constraints.[3, 12] Also, we have previously shown that epithelial cells can exhibit directional movement on teardrop-based micropatterns.[5] This study focused on the potential to combine the enhanced speed and persistence on line patterns and the directional bias provided by the teardrop-based patterns for MCF-10A epithelial cells. The cell motility on this hybrid, spear-shaped pattern was found to exceed that on both of the original patterns and was quantitatively analyzed to understand the cause of the

enhancements. Furthermore, this hybrid pattern with enhanced motility was applied to partition designs to optimize the partition efficiencies of cell population, significantly surpasses that reported in previous works.[11] Thus, this study demonstrates the ability to effectively combine motifs of micropatterns to create hybrid patterns with synergistic outcomes and sheds light on the vast, underlying potentials in micropatterning technology.

## 5. Experimental Methods

### *5.1. Fabrication of micropatterned substrates*

Microcontact printing with a polydimethylsiloxane (PDMS) stamp was used to pattern the adhesion ligand, as described previously.[5] Briefly, UV light is passed through a chrome mask containing the teardrop and spear-shaped patterns (Nanoelectronics Research Facility, UCLA) onto a layer of SU-8 negative photoresist to make a mold, onto which PDMS is cast to make the stamp. 16-Mercaptohexadecanoic acid (Sigma Aldrich) was printed with the stamp onto the gold-coated chambered coverslide (Fisher Thermo Scientific – NUNC). The unprinted area is passivated using PEG(6)-Thiol (Prochimia) so as to prevent protein adsorption and cell adhesion. The acid was then covalently bound to fibronectin to make cell adhesive patterns. Finally, BSA conjugated with Alexa Fluor 594 (Invitrogen) was doped to visualize the patterns (Chapter II Figure S4).

*5.2. Cell culture*

MCF-10A human epithelial cells were cultured in growth medium composed of Dulbecco's modified Eagle's medium/Ham's F-12 containing HEPES and L-glutamine (DMEM/F12, Invitrogen) supplemented with 5% horse serum (Invitrogen), 1% penicillin/streptomycin, 10µg/mL insulin (Sigma), 0.5µg/mL hydrocortizone (Sigma), 20ng/mL EGF (Peprotech) and 0.1µg/mL cholera toxin (Sigma) and maintained under humidified conditions at 37 ºC and 5% $CO_2$. Cells were passaged regularly by dissociating confluent monolayers with 0.05% trypsin-EDTA (Invitrogen) and suspending cells in DMEM/F12 supplemented with 20% horse serum and 1% penicillin/streptomycin. After two washes, cells were diluted 1:4 and plated in growth medium.

*5.3. Timelapse microscopy*

Cells were seeded in growth medium for 1h onto the micropatterned substrate. After washing to remove non-adherent cells, the culture was incubated with fresh growth medium for 1 hr and imaged at 10x magnification every 5min for 12hr (for single cell analysis) or every 3 hours for 36 hours (for multicellular analysis on partition patterns). Cells were maintained at 37ºC and 5% $CO_2$ in a heated chamber with temperature and $CO_2$ controller (Pecon) during time-lapse imaging. Images and movies were acquired using Axiovert 200M microscope (Carl Zeiss), and Axio Vision LE Rel. 4.7 (Carl Zeiss) was used for image analysis.

*5.4. Data collection and analysis*

For line patterns, the lamellipodial position was tracked using Axio Vision LE Rel. 4.7 and ImageJ software. Migration speed was obtained as the total distance traveled divided by the total time. The persistence length was based on switching the direction 180° and also on whether unilamellar morphology was broken or not (i.e., if a cell paused to spread and then eventually proceeded in the same direction, it was counted as a separate run).

For the speed and persistence calculation on classic teardrop and spear-shaped pattern analysis, a few assumptions were made. We assumed that for a cell to hop from one island to another island, it must travel 80 μm across the normal teardrop island and 180 μm across the spear-shaped island, and hop sideways across a 3 μm gap. If a cell starts or ends in the middle of an island, a method similar to line patterns were used to determine the auxiliary distance. Also, the residence times at each corner for each scenario (to hop or not to hop) were tracked separately; cells were considered as resident at a corner until their trailing edge was completely detached from that corner.

For the partition patterns, cells in the upper half of the pattern (one image) and the lower part of the pattern (another image) were counted for each pattern (cells that overlap between both images were considered as upper half). The data was expressed as percentages to account for the proliferation of cells. The bridge section was included because it is where a significant portion of the cells can reside (up to 70%) and also the most dynamic area of the pattern.

## 6. Acknowledgements

*This research was funded by the NSF Center for Science and Engineering of Materials at Caltech. We also gratefully acknowledge the technical support and infrastructure provided by the Kavli Nanoscience Institute.*

## 7. References

[1] D. M. Brunette, *Exp Cell Res* **1986**, *167*, 203.

[2] P. Clark, P. Connolly, A. S. Curtis, J. A. Dow, C. D. Wilkinson, *J Cell Sci* **1991**, *99 ( Pt 1)*, 73.

[3] A. D. Doyle, F. W. Wang, K. Matsumoto, K. M. Yamada, *J Cell Biol* **2009**, *184*, 481.

[4] G. Kumar, C. C. Ho, C. C. Co, *Advanced Materials* **2007**, *19*, 1084.

[5] K. Kushiro, S. Chang, A. R. Asthagiri, *Advanced Materials* **2010**, n/a. doi: 10.1002/adma.201001619

[6] P. P. Provenzano, D. R. Inman, K. W. Eliceiri, S. M. Trier, P. J. Keely, *Biophys J* **2008**, *95*, 5374.

[7] E. Sahai, *Nat Rev Cancer* **2007**, *7*, 737.

[8] P. Clark, S. Britland, P. Connolly, *J Cell Sci* **1993**, *105 ( Pt 1)*, 203.

[9] D. Gao, G. Kumar, C. Co, C. C. Ho, *Adv Exp Med Biol* **2008**, *614*, 199.

[10] B. Szabo, Z. Kornyei, J. Zach, D. Selmeczi, G. Csucs, A. Czirok, T. Vicsek, *Cell Motil Cytoskeleton* **2004**, *59*, 38.

[11] G. Mahmud, C. J. Campbell, K. J. M. Bishop, Y. A. Komarova, O. Chaga, S. Soh, S. Huda, K. Kandere-Grzybowska, B. A. Grzybowski, *Nature Physics* **2009**, *5*, 606.

[12] D. Irimia, M. Toner, *Integr Biol (Camb)* **2009**, *1*, 506.